NeuroReport 10, 3711–3716 (1999)

Potentiation of Ca^{2+} influx through NMDA channels by action potentials: a computer model

Kevin R. Neville[1] and William W. Lytton[1,2,CA]

[1]Neuroscience Training Program and [2]Department of Neurology, University of Wisconsin-Madison, 1300 University Ave, Madison, WI 53706, USA

[CA]Corresponding Author

IN pyramidal cells, somatic action potentials can propagate actively back into the apical dendrites and potentiate calcium influx at simultaneously activated glutamatergic synapses, presumably by relieving the voltage-dependent block of NMDA channels. We have used computer simulations to investigate the conditions under which this potentiation will be optimal. We find that a spike with a long duration and limited amplitude (peak of ~ -10 mV) will be most effective. A backpropagating action potential will achieve this form if the dendritic membrane has a low K^+ channel density and a modest Na^+ channel density (30–70 pS/μm^2, similar to experimentally observed densities). The relative increase in calcium due to the backpropagating spike will be small, however, unless the accumulated calcium is rapidly removed. *NeuroReport* 10:3711–3716

Key words: Action potentials; Backpropagation; Calcium; Dendrites; long-term potentiation; NMDA receptors; Pyramidal cells

Introduction

Half a century ago, Hebb [1] proposed that a network of cells could store information by increasing the strength of synapses when a presynaptic cell repeatedly took part in causing a postsynaptic cell to fire. Interest has focused on the phenomenon of long-term potentiation (LTP), some forms of which require calcium influx through NMDA-type glutamate receptors. NMDA channels are largely blocked by extracellular Mg^{2+} ions at resting membrane potential, so a depolarization of the postsynaptic membrane coincident with receptor activation will greatly increase the calcium influx. Recent experiments have demonstrated that an action potential initiated in the soma or axon can propagate actively back into the apical dendritic tree of a hippocampal or neocortical pyramidal cell [2,3]. Thus, the removal of the Mg^{2+} block by a backpropagating action potential, with increased calcium inducing LTP, could be a mechanism for Hebbian plasticity. Indeed, calcium imaging studies have indicated that either synaptic activation or a backpropagating action potential can generate an increase in dendritic calcium concentrations, but the combination of both can elicit a supralinear calcium accumulation [4–7] and induce synaptic plasticity [5,8–9].

Questions remain as to the conditions under which this mechanism will be significant and the means by which it might be regulated. The amplitude and duration of the depolarization provided by a backpropagating action potential will depend on the active conductances present in the dendritic membrane, which are subject to modification and regulation. Here, we have used computer simulations to investigate the ability of a backpropagating action potential to potentiate calcium influx through NMDA channels by relieving the voltage-dependent Mg^{2+} block. For simplicity, we have restricted our investigations to the interaction of a single action potential with a single, weak excitatory synapse located on a distal branch of the apical dendrite. By systematically varying the densities of active dendritic conductances, we sought to determine the conditions under which this interaction will be most significant and thereby to identify possible means of regulation.

Materials and Methods

All simulations were performed using Neuron [10]. A timestep of 10 μs was used throughout. The simulated temperature was 23°C to match the kinetics reported for various channels at room temperature. Neuronal morphology came from Kapur *et al.* [11]. A layer II pyramidal cell of rat piriform cortex was filled with Neurobiotin, sectioned and traced. The model consisted of 345 compartments, each ≤ 35 μm in length. A single excitatory synapse was placed on the shaft of a distal apical dendrite 366 μm from the soma.

Passive membrane properties used were

$R_i = 137\ \Omega\cdot cm$, $R_m = 14\,005\ \Omega/cm^2$ and $C_m = 1.49\ \mu F/cm^2$, as determined for this cell by fitting whole-cell voltage transient recordings [11]. Simulations usually included a fast voltage-gated sodium channel (Na_F) and either a delayed rectifier (K_{DR}) or A-type potassium channel (K_A) or both. All voltage-gated channels were simulated with a Hodgkin-Huxley form: $I = g_{max} \times m^n \times h \times (v - E_{rev})$ $dm/dt = m_\alpha \times (1-m) - m_\beta \times m = (m^\infty - m)/\tau_m$ $dh/dt = h_\alpha \times (1-h) - h_\beta \times h = (h^\infty - h)/\tau_h$

Parameters for Na_F were fit to reproduce physiological data from neocortical and hippocampal pyramidal cells, with particular care paid to the time constant of inactivation. For the fast sodium current, $E_{rev} = 60$ mV, $n = 3$ $m_\alpha = -0.32 \times (v + 54)/\{\exp[(v + 54)/-6] - 1\}$; $m_\beta = 0.28 \times (v + 31)/\{\exp[(v + 31)/6] - 1\}$ $h_\alpha = 0.2 \times \exp[(v + 105)/-20]$; $h_\beta = 2/\{\exp[(v + 22)/-10] + 1\}$

The parameters for the transient potassium current K_A were fit to the data of Banks *et al.* [12] for layer II pyramidal cells of piriform cortex.

$E_{rev} = -75$ mV, $n = 3$ $m_\alpha = 0.5 \times \exp[(v + 46)/30.8]$; $m_\beta = 0.5 \times \exp[(v + 46)/30.8]$ $h_\alpha = 0.07 \times \exp[(v + 55.5)/-7.11]$, $h_\beta = 0.07 \times \exp[(v + 55.5)/64]$

Two descriptions of slowly inactivating potassium current K_{DR} were used, one with $n = 1$($_{KDR}1$), and the other with $n = 4$($_{KDR}4$). Inactivation was not included for these conductances. For $K_{DR}1$, $E_{rev} = -75$ mV, $n = 1$ $m_\alpha = -0.00325 \times (v + 15)/\{\exp[(v+15)/-5] - 1\}$, $m_\beta = 0.05 \times \exp[(v + 30)/-40]$

For $K_{DR}4$, $E_{rev} = -75$ mV, $n = 4$ $m_\alpha = -0.008 \times (v + 35)/\{\exp[(v + 35)/-5] - 1\}$ $m_\beta = 0.06 \times (v + 50)/\{\exp[(v + 50)/-40] - 1\}$

A constant density of 100 mS/cm^2 Na_F channels were placed in the soma, along with 20 mS/cm^2 $K_{DR}4$ and 60 mS/cm^2 K_A. Current injection into the soma (3 nA for 1 ms) evoked a single action potential which matched the peak height (90 mV from a resting potential of −65 mV), width at half height (0.9 ms), and width at one quarter height (1.4 ms) of the action potentials recorded from a layer II piriform pyramidal cell *in vitro* at 24°C.

The AMPA component of the synaptic current (in nA) starting at time $t = 0$ ms was modeled as: $I = 400\ pS \times (v - 0\ mV) \times [1 - \exp(-t/0.1\ ms)]$ for $t < 0.5$ ms; $I = 400\ pS \times (v - 0\ mV) \times \exp[-(t - 0.5\ ms)/2\ ms]$ for $t > 0.5$ ms.

The NMDA component of the synaptic current (in nA) starting at time $t = 0$ ms was modeled as: $I = 150\ pS \times [1 - \exp(-t/2ms)]/[1 + 0.28 \times \exp(-0.063 \times v)] \times (v - 3\ mV)$ for $t < 10$ ms; $I = 150\ pS \times \exp[-(t - 10\ ms)/67\ ms]/[1 + 0.28 \times \exp(-0.063 \times v)] \times (v - 3\ mV)$ for $t > 10$ ms.

To model the Ca^{2+} influx through an NMDA synapse, the Goldman–Hodgkin–Katz equation was used. This required the use of a conversion factor P_x to relate the permeability for calcium to the total channel conductance g. This factor was determined empirically such that ~10% of the current would be carried by Ca^{2+} at −40 mV, and corresponds to a permeability ratio $P_{Ca}:P_{Na}:P_K = 3:1:1$.

$I_{Ca} = -g \times P_x \times 4 \times v \times F^2/(R \times T) \times \{[Ca]_o \times \exp[-2 \times v \times F/(R \times T)] - [Ca]_i\}/\{1 - \exp[-2 \times v \times F/(R \times T)]\}$ with $P_x = 0.0046925$ (V·cm^3/Coul), $F = 96.49$ kCoul/mol, $R = 8.314$ J/K/mol, $[Ca]_o = 1.5$ mM, and $[Ca]_i = 50$ nM. The accumulated Ca^{2+} was computed as the integral of the Ca^{2+} current over the duration of the simulation, typically 100 ms. Except in Fig. 1, a time constant of decay for the accumulated calcium was included, called τ_{Ca}. Thus d(accumulated calcium)/dt = I_{Ca} −(accumulated calcium)/τ_{Ca}.

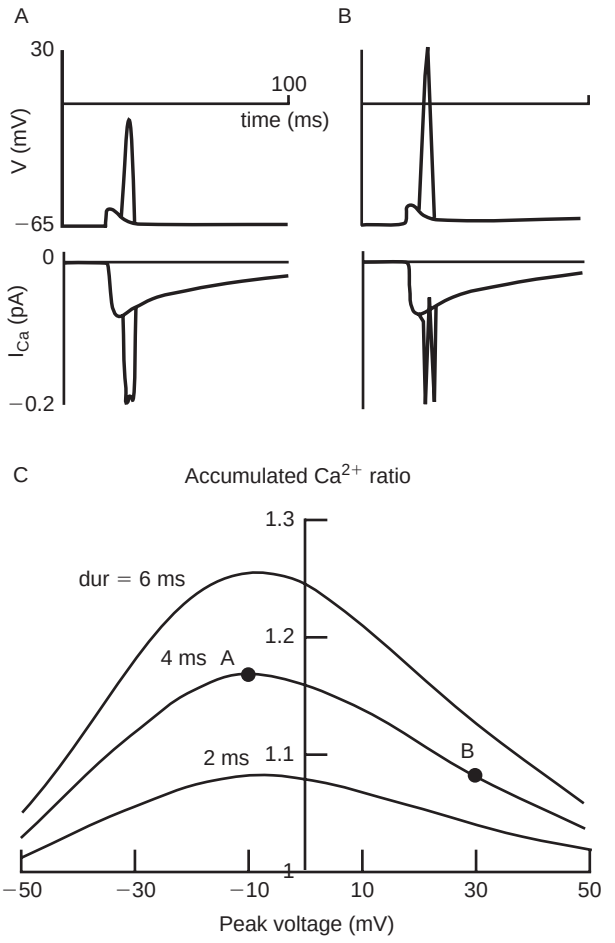

FIG. 1. Calcium influx dependence on spike height and duration at the postsynaptic membrane. Voltage at the synapse and NMDA-mediated calcium currents. (**A**,**B**) Heavy traces, voltage and calcium current due to the synaptic conductance alone. Light traces, voltage waveform imposed on the postsynaptic membrane, and the resulting calcium current. Note that the calcium current was reduced with the larger amplitude waveform (spike height +30 mV in B, −10 mV in A), as the driving force on calcium was reduced. Spike duration was 4 ms at half amplitude. (**C**) Potentiation of total calcium influx by a postsynaptic voltage peak. For each choice of peak voltage and duration, the calcium current was integrated. Total accumulated calcium with the spike is shown, normalized by the total calcium influx due to the EPSP alone. The specific choices of spike height and duration used in (A) and (B) are indicated.

Typically two identical cells were simulated, one with a spike and one without. The ratio of the peak accumulated Ca^{2+} in the cell with the spike to the peak accumulated Ca^{2+} in the cell without one is referred to as the potentiation of accumulated Ca^{2+} by the spike.

Results

We first investigated the effect of a spike in the postsynaptic membrane voltage on NMDA-mediated calcium influx. For the control condition, a single excitatory synapse on a distal dendrite was simulated, generating a 10 mV local EPSP and 0.07 pA of calcium current (Fig. 1A,B, dark traces). The simulation was repeated with the postsynaptic membrane clamped to a voltage waveform which combined the EPSP with a spike of specified amplitude and duration (Fig. 1A,B, light traces). The calcium component of the NMDA current was recorded (Fig. 1A,B, lower traces) and integrated to obtain the total accumulated calcium in each condition. The accumulated calcium with the imposed voltage spike was normalized by the accumulated calcium in the control condition to determine the potentiation of accumulated calcium by the spike. Figure 1C shows the dependence of potentiation on the height of the spike for three different durations. Two trends were seen. First, potentiation of accumulated calcium was always greater for spikes of longer duration. Second, for any given duration, potentiation was maximal when the height of the spike was ~−10 mV. Below this level, the NMDA conductance was not fully unblocked, while spikes which exceeded this optimum reduced the driving force on calcium.

The potentiation in Fig. 1 appeared rather limited: the most effective spike tested increased calcium accumulation by only 26%. This was because the NMDA conductance greatly outlasted the voltage spike, and the NMDA channel was not fully blocked at resting potential, so that even when the membrane potential had returned to rest, some calcium continued to enter. Most of the calcium, in fact, entered during the long tail of the EPSC. We postulated that integration over a shorter time window would improve the ability of a spike to potentiate calcium influx. We therefore introduced a time constant of decay for the accumulated calcium, called τ_{Ca}, and compared the peak calcium accumulation reached with and without a postsynaptic voltage spike. Figure 2A shows the accumulated

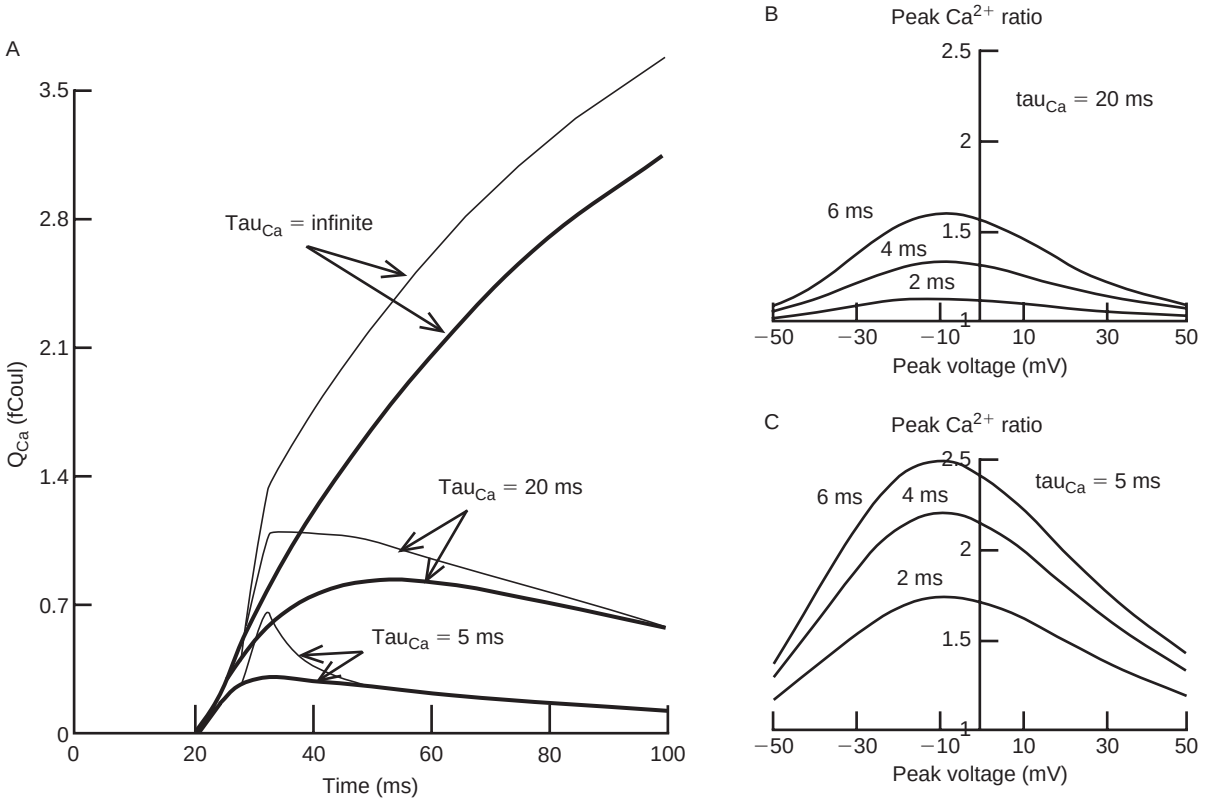

FIG. 2. Effects of the calcium decay parameter, τ_{Ca}. (**A**) Accumulated calcium as a function of time. Calcium was added by the ongoing calcium current and removed with a decay time constant of τ_{Ca}. Heavy traces: synaptic conductance alone. Light traces: with imposed spike (−10 mV peak voltage, 4 ms duration, as in Fig. 1A). Three values of τ_{Ca} are shown. (**B**,**C**) Potentiation of peak accumulated calcium by a spike with different values of τ_{Ca} (B, τ_{Ca} = 20 ms; C, τ_{Ca} = 5 ms; compare with Fig. 1C where τ_{Ca} = infinite; note the different scales). For each choice of spike height and duration, the peak accumulated calcium with the spike is shown, normalized by the peak accumulated calcium due to the EPSP alone.

calcium as a function of time, both with an imposed spike (light traces) and without (dark traces) for several values of τ_{Ca}. The spike caused a brief, steep rise in accumulated calcium. Thereafter, with a long τ_{Ca}, calcium continued to accumulate at a similar rate in both the control condition (EPSP alone) and with the added spike, and the final ratio of peak calcium was only slightly greater than unity. With a short τ_{Ca}, however, the slow influx of calcium during the tail of the EPSC was offset by the calcium decay, and the accumulated calcium in the control condition never reached the peak level of accumulated calcium with the spike. The potentiation of peak calcium was therefore greater with a shorter time constant of calcium decay (Fig. 2B,C).

We next addressed the effect of active dendritic conductances on the shape of a backpropagating action potential. Two identical cells were modeled: the first with a synaptic conductance only, and the second with both a synaptic conductance and a current injection into the soma sufficient to produce a single action potential (3 nA for 1 ms, 5 ms after the start of the synaptic conductance). Figure 3 shows the resulting voltage waveforms at the soma, the synapse, and two locations in between for the cell with the EPSP alone (dark traces) or the EPSP plus an action potential (light traces). With passive dendrites (left column), the action potential attenuated greatly. With increasing dendritic Na^+ and K^+ channel densities, the action potential at the synapse increased in height, but also became narrower. The greater Na^+ channel density led to a faster rate of rise and a higher peak, which in turn resulted in faster Na^+ channel inactivation and K^+ channel activation. In parameter sensitivity experiments, a shift in the voltage dependence of activation or inactivation to more depolarized potentials produced effects that were qualitatively similar to the effects of reducing the peak conductance, for both Na^+ and K^+ channels (data not shown).

The potentiation of peak accumulated calcium by a backpropagating action potential is shown as a contour plot in Fig. 4, as a function of the densities of dendritic Na^+ and K^+ channels. Not surprisingly, a higher density of K^+ channels reduced the ability of the backpropagating action potential to potentiate peak calcium accumulation. The less intuitive result, however, was that for any given density of K^+

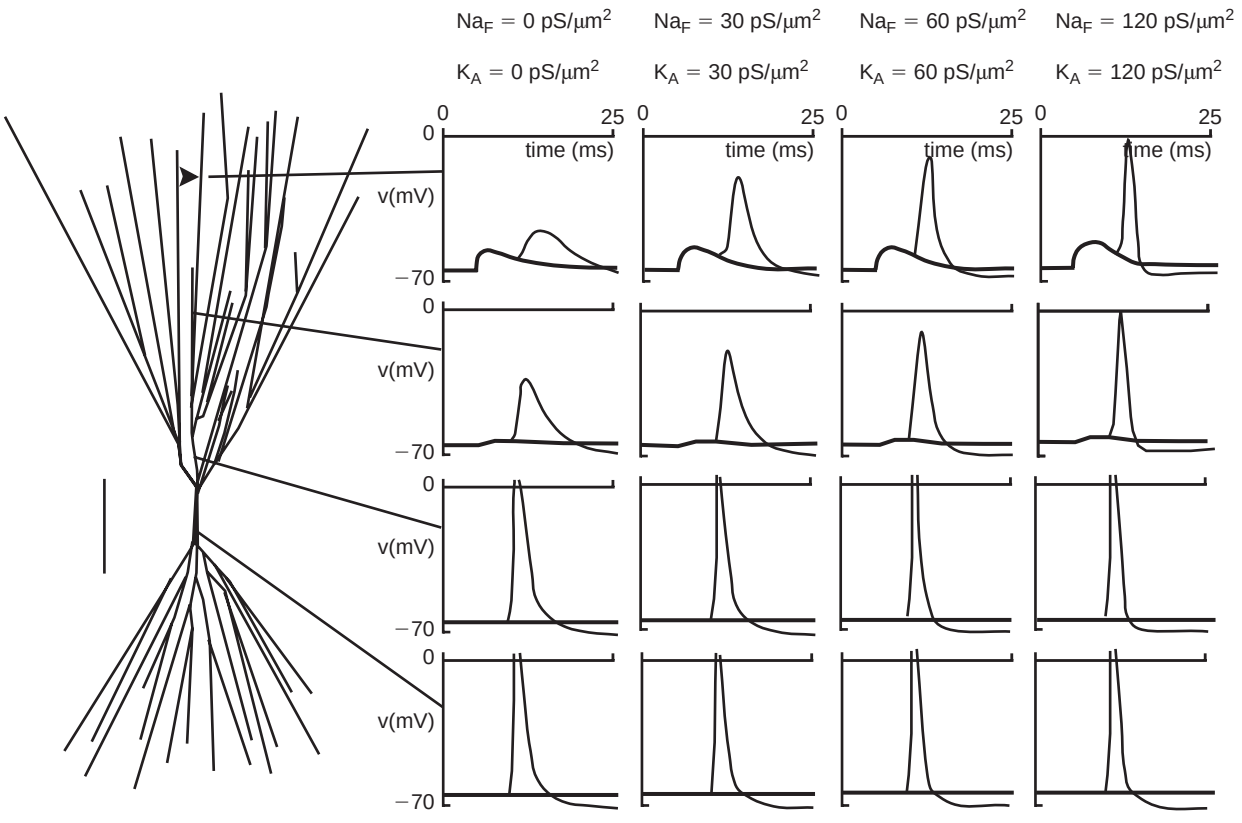

FIG. 3. The influence of active dendritic conductances on the shape of a back-propagating action potential. The model neuron is illustrated schematically at left, with recording sites indicated. Arrowhead indicates location of synapse. Bar = ~100 μm. Heavy traces: voltage due to the synaptic conductance alone. Light traces: voltage with the synaptic conductance plus an action potential evoked by somatic current injection (3 nA, 1 ms). Each row is a different recording location (top row, location of synapse). Each column is a different density of dendritic channels: left to right, $g_{NaF} = g_{KA} = 0$ pS/μm², $g_{NaF} = g_{KA} = 30$ pS/μm², $g_{NaF} = g_{KA} = 60$ pS/μm², $g_{NaF} = g_{KA} = 120$ pS/μm²

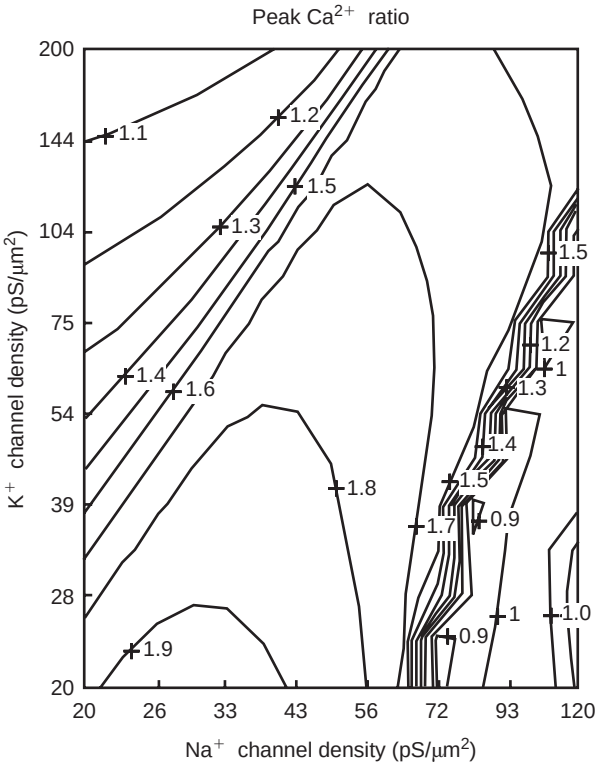

FIG. 4. Potentiation of peak accumulated calcium by a back-propagating action potential. Peak NMDA-mediated calcium accumulation ($\tau_{Ca} = 5$ ms) with a somatic action potential was normalized by the peak calcium accumulation due to the EPSP alone. These ratios were computed for each density of Na^+ and K^+ channels, and are displayed as a contour plot. At the highest Na^+ channel densities and lowest K^+ channel densities, synaptic input alone evoked an action potential, resulting in negligible potentiation by the addition of a somatic current injection.

channels, there was an optimal density of dendritic Na^+ channels. Fewer Na^+ channels produced an action potential whose amplitude was too small to effectively unblock NMDA channels, while more Na^+ channels produced an action potential whose duration was too brief, such that the NMDA channels were unblocked only momentarily. Depending on the density and type of K^+ channels included in the model, the optimal Na^+ channel density was 30–70 pS/μm², similar to experimentally determined densities in apical dendrites of hippocampal and neocortical cells [13,14]. The results shown in Fig. 4 assumed a uniform distribution of Na^+ and A-type K^+ channels. Simulations with a non-inactivating K^+ conductance, a non-uniform distribution of A-type channels (increasing linearly with distance from the soma [15]), or both all produced qualitatively similar results (data not shown): a backpropagating action potential could best potentiate the peak accumulated calcium if the dendrites contained a low density of K^+ channels and a modest density of Na^+ channels.

Discussion

The coincidence of pre- and postsynaptic activity has long been hypothesized to result in synaptic plasticity [1]. The NMDA receptor, with its high calcium permeability and voltage dependence, has become a primary focus of attention in the search for a mechanism which may underlie such plasticity. Traditionally, the postsynaptic depolarization was presumed to be provided by other simultaneously active synaptic inputs, so-called hetero-associative LTP. Recently an alternative has emerged: a back-propagating action potential may provide the depolarization required to remove the Mg^{2+} block of NMDA channels. These two mechanisms implement very different computational algorithms. The first links synaptic plasticity to converging input, regardless of whether or not that input successfully drives the cell to fire. The second proposed mechanism, which we have investigated here, requires the presynaptic cell to participate in driving the postsynaptic cell to fire, and is thus closer to Hebb's original proposal.

Our simulations have focused on the pairing of a single synaptic input with a single backpropagating action potential. The common LTP-inducing protocol employing tetanic stimuli is more complex. Both Na^+ and K^+ channels will inactivate with prolonged depolarization, while the synaptic bombardment will provide a greater depolarization of the postsynaptic membrane, possibly reducing the need for backpropagating spikes. Our simulations are analogous to the experiments of Markram *et al.* [9] using dual impalements of monosynaptically connected neocortical pyramidal cells. These authors evoked LTP by repeatedly pairing single pre- and postsynaptic action potentials. Likewise, Koester and Sakmann [6] paired single EPSPs and action potentials to evoke supralinear calcium accumulation in individual spines.

Direct recordings from the dendrites of neocortical and CA1 hippocampal pyramidal cells indicate that an action potential initiated at the soma will decrement and broaden as it propagates back into the apical dendrite. Generally, *in vitro* reports agree that in the distal portions of the dendrite, such an action potential will have an amplitude of 45–60 mV and a duration of 2–4 ms at physiological temperature [5,15-17], or a duration of ~7 ms at room temperature [13]. Figure 1 shows that these amplitudes (corresponding to peak voltages of −20 to 0 mV) are nearly optimal for the potentiation of calcium influx through NMDA channels. Dendritic action potentials recorded *in vivo* [18] have greatly reduced amplitude, however. Likewise, later action potentials in a train *in vitro* decrement to a much

greater extent than the first spikes [16,19,20], an effect that can be prevented by muscarinic inputs [21]. It thus appears that pyramidal cell dendrites are capable of supporting action potentials of the optimal amplitude for interaction with NMDA channels, but the actual amplitude may be under the control of modulatory inputs.

These simulations show that the ability of a backpropagating action potential to potentiate the peak calcium level depends critically on the time window over which the influx is integrated. We have represented this limited time window with the time constant τ_{Ca}, representing the rapid clearance of accumulated intracellular calcium. A short τ_{Ca} will favor the action potential–NMDA interaction by filtering out the slow background influx during the tail of the EPSC. Initial imaging studies of calcium transients in single spines used high-affinity calcium dyes and reported a decay time constant of $\geqslant 150$ ms [4,6], but the buffering action of these dyes can be expected to significantly prolong the timecourse of transient calcium signals. A quantitative study of this effect yielded a time constant between 50 and 100 ms in the shafts of apical dendrites of neocortical and hippocampal cells [22]. Most recently, Yuste *et al*. [7] have used both high- and low-affinity calcium dyes to image calcium transients in spines evoked by backpropagating action potentials. With the low-affinity dye, the time constant of decay of the calcium transient was reduced to ~20 ms (see their Fig. 7). This value of τ_{Ca} is fast enough for an action potential to effectively potentiate peak calcium levels due to influx through NMDA channels (Fig. 2). The fast clearance of calcium from the spine head compared to the dendritic shaft could be due to a greater surface-to-volume ratio or specialized mechanisms for the removal or sequestration of calcium.

Both Na^+ and K^+ channels are subject to extensive regulation and modulation [23,24]. We therefore treated the densities of these conductances in the dendritic membrane as free parameters. Our simulations showed that the shape of the action potential in the distal dendrite, and therefore its ability to potentiate calcium influx through NMDA channels, was indeed sensitive to the densities of Na^+ and K^+ conductances in the dendritic membrane (Fig. 3, Fig. 4). The action potential was most effective when the dendrites contained a low density of K^+ channels and a modest density of Na^+ channels. The optimal density of Na^+ channels (30–70 pS/μm^2) for this phenomenon agrees remarkably well with the density of Na^+ channels reported for patch recordings from pyramidal cell dendrites in hippocampus (61 pS/μm^2 in adult rats, 28 pS/μm^2 in juveniles) [14] and neocortex (40 pS/μm^2 in 2-week-old rats) [13]. This suggests that these cells may be optimized to support the interaction of action potentials with NMDA receptors. It also suggests that further increasing the dendritic Na^+ conductance will not improve this interaction. Instead, the dendritic K^+ conductance must be reduced. This is in keeping with the proposed importance of the A-type K^+ channel in regulating dendritic excitability and associative plasticity [3,15,16,23].

Conclusion

Postsynaptic action potentials can interact with synaptic input to generate supralinear calcium transients [4–7] and long-term potentiation [5,8,9]. In this paper, we have examined the dependence of this interaction on the dendritic membrane properties and calcium integration time window. We have demonstrated that a postsynaptic spike will be most effective at potentiating peak calcium levels if that spike has a long duration and a peak voltage of ~−10 mV. An action potential initiated at the soma and propagating back into the dendrites will achieve this optimal form if the dendritic membrane contains a low density of K^+ channels and a modest density of Na^+ channels. The spike will only be effective, however, if the calcium influx is integrated over a relatively brief time window ($\tau_{Ca} \leqslant 20$ ms). Experimental measures of dendritic Na^+ channel density match the optimum reported here [13,14], and the clearance of calcium from spines does appear to be fast [7], suggesting that pyramidal cells may be optimized to make use of this mechanism.

References

1. Hebb DO. *The Organization of Behavior*. New York: Wiley, 1949.
2. Stuart G, Spruston N, Sakmann B *et al. Trends Neurosci* **20**, 125–131 (1997).
3. Magee J, Hoffman D, Colbert C *et al. Ann Rev Physiol* **60**, 327–346 (1997).
4. Yuste R and Denk W. *Nature* **375**, 682–684 (1995).
5. Magee JC and Johnston D. *Science* **275**, 209–212 (1997).
6. Koester HJ and Sakmann B. *Proc Natl Acad Sci USA* **95**, 9596–9601 (1998).
7. Yuste R, Majewska A, Cash SS *et al. J Neurosci* **19**, 1976–1987 (1999).
8. Jester JM, Campbell LW and Sejnowski TJ. *J Physiol (Lond)* **484**, 689–705 (1995).
9. Markram H, Lubke J, Frotscher M *et al. Science* **275**, 213–215 (1997).
10. Hines M. *Int J Biomed Comput* **24**, 55–68 (1989).
11. Kapur A, Lytton WW, Ketchum KL *et al. J Neurophysiol* **78**, 2546–2559 (1997).
12. Banks MI, Haberly LB and Jackson MB. *J Neurosci* **16**, 3862–3876 (1996).
13. Stuart GJ and Sakmann B. *Nature* **367**, 69–72 (1994).
14. Magee JC and Johnston D. *J Physiol (Lond)* **487**, 67–90 (1995).
15. Hoffman DA, Magee JC, Colbert CM *et al. Nature* **387**, 869–875 (1997).
16. Andreasen M and Lambert JDC. *J Physiol (Lond)* **483**, 421–441 (1995).
17. Stuart G, Schiller J and Sakmann B. *J Physiol (Lond)* **505**, 617–632 (1997).
18. Kamondi A, Acsady L and Buzsaki G. *J Neurosci* **18**, 3919–3928 (1998).
19. Spruston N, Schiller Y, Stuart G *et al. Science* **268**, 297–300 (1995).
20. Callaway JC and Ross WN. *J Neurophysiol* **74**, 1395–1403 (1995).
21. Tsubokawa H and Ross WN. *J Neurosci* **17**, 5782–5791 (1997).
22. Helmchen F, Imoto K and Sakmann B. *Biophysical J* **70**, 1069–1081 (1996).
23. Hoffman DA and Johnston D. *J Neurosci* **18**, 3521–3528 (1998).
24. Li M, West JW, Numann R *et al. Science* **261**, 1439–1442 (1993).

ACKNOWLEDGEMENTS: W.W.L. was supported by NIH Grant NS32187. K.R.N. was supported by a UW WARF Fellowship and a Howard Hughes Predoctoral Fellowship. We thank Drs Lewis Haberly, Robert Pierce, Larry Trussel, and Robert Fettiplace for helpful discussions.

Received 29 July 1999; accepted 24 September 1999